Published in final edited form as:
Mol Cell. 2010 October 28; 40(3): 364–376. doi:10.1016/j.molcel.2010.10.011.

Regulation of the Histone H4 Monomethylase PR-Set7 by CRL4^{Cdt2} Mediated PCNA Dependent Degradation during DNA Damage

Hisanobu Oda[2,6], **Michael R. Hübner**[3,6], **David B. Beck**[2], **Michiel Vermeulen**[4], **Jerard Hurwitz**[5], **David L. Spector**[3], and **Danny Reinberg**[1,2]

[1]Howard Hughes Medical Institute, New York University School of Medicine, 522 First Avenue, New York, New York 10016, USA [2]Department of Biochemistry, New York University School of Medicine, 522 First Avenue, New York, New York 10016, USA [3]Cold Spring Harbor Laboratory, One Bungtown Road, Cold Spring Harbor, New York 11724, USA [4]Department of Physiological Chemistry and Cancer Genomics Centre, University Medical Center Utrecht, 3584 CG Utrecht, The Netherlands [5]Program of Molecular Biology, Memorial Sloan-Kettering Cancer Center, New York, New York 10065, USA

Abstract

The histone methyltransferase PR-Set7/Set8 is the sole enzyme that catalyzes monomethylation of histone H4 at lysine 20 (H4K20me1). Previous reports document disparate evidence regarding PR-Set7 expression during the cell cycle, the biological relevance of PR-Set7 interaction with PCNA, and its role in the cell. We find that PR-Set7 is indeed undetectable during S phase and instead is detected during late G2, mitosis and early G1. PR-Set7 is transiently recruited to laser-induced DNA damage sites through its interaction with PCNA, after which 53BP1 is recruited dependent on PR-Set7 catalytic activity. During the DNA damage response, PR-Set7 interaction with PCNA through a specialized “PIP degron” domain targets it for PCNA-coupled CRL4^{Cdt2} dependent proteolysis. PR-Set7 mutant in its “PIP degron” is now detectable during S phase during which the mutant protein accumulates. Outside the chromatin context, Skp2 promotes PR-Set7 degradation as well. These findings demonstrate a stringent spatiotemporal control of PR-Set7 that is essential for preserving the genomic integrity of mammalian cells.

Introduction

Distinct histone post-translational modifications are now being recognized as being causally related to the formation of different chromatin structural domains that are either conducive to or inhibitory to processes that necessitate DNA access (Kouzarides, 2007; Li et al., 2007; Margueron et al., 2005). The means by which these modifications are successfully incorporated, the changes these modifications elicit in chromatin structure, and how these processes are regulated are key areas of intense study (Campos and Reinberg, 2009). One such histone modification is monomethylation of histone H4 at lysine residue 20

Correspondence to: Danny Reinberg.

[6]These authors contributed equally to this work.

(H4K20me1). H4K20me1 catalysis is completely dependent on the activity of PR-Set7 and requires its SET domain (Nishioka et al., 2002; Oda et al., 2009). However, H4K20 is not the only target of PR-Set7 as the tumor suppressor protein p53 is also methylated at lysine residue 382 resulting in suppression of p53 dependent transcriptional activation (Shi et al., 2007).

The H4K20me1 mark is associated with transcriptionally repressed, compacted chromatin. It is also a mark to which 53BP1 binds through its double-tudor domains, a function that is conserved in *Schizosaccharomyces pombe* (Botuyan et al., 2006; Sanders et al., 2004). It is postulated that 53BP1 binding to sites of DNA damage facilitates a sequence of events in DNA repair, though the mechanisms are not totally elucidated and the determinant(s) for targeting 53BP1 to DNA damage sites has not been established (FitzGerald et al., 2009).

The biological impact of PR-Set7 activity was demonstrated using a knockout mouse model (Oda et al., 2009). Embryonic lethality was evident by the four-cell stage of embryogenesis. This phenotype was rescued upon injection of mRNA encoding WT (wild-type), but not a SET domain mutant of PR-Set7, highlighting the importance of its enzymatic activity during embryogenesis (Oda et al., 2009). Our previous results demonstrated that PR-Set7 normally exhibits a strict pattern of cell cycle regulated expression (Oda et al., 2009; Rice et al., 2002). PR-Set7 was undetectable during DNA replication in S phase of the cell cycle and, instead, was clearly evident starting during late G2 and in mitosis at which time PR-Set7 was associated with post-replicative chromosomes. H4K20me1 was found to be important for chromosome integrity and compaction (Oda et al., 2009). Our previous studies demonstrated two additional phenotypes upon PR-Set7 inactivation. ES cells lacking PR-Set7 displayed aberrant chromosome condensation as well as massive DNA damage as detected by the recruitment of γH2A.X (Oda et al., 2009). Interestingly, embryos devoid of PR-Set7 failed to develop beyond the four-cell stage, but did not display DNA damage (Oda et al., 2009).

PR-Set7 has been reported as containing two PIP (PCNA Interacting Protein) domains (Huen et al., 2008; Jorgensen et al., 2007) that confer binding to PCNA (Proliferating Cell Nuclear Antigen), a protein clamp that ensures processive DNA synthesis during replication and repair (Moldovan et al., 2007). In light of these studies based on PCNA/PR-Set7 interaction, it was suggested that PR-Set7 is present during S-phase and that it is required specifically for the stability and the replication of the genome (Jorgensen et al., 2007). It was also suggested that the possible substrate for PR-Set7 methyltransferase during S phase is the DNA replication machinery (Tardat et al., 2007). We initiated the studies herein to resolve the controversy of the presence of PR-Set7 during the cell cycle and its putative role in DNA replication. As we previously found, PR-Set7 is not detectable in S-phase. Our findings show that this enzyme is degraded in G1, several hours before the start of DNA replication. Moreover, it is PR-Set7 interaction with PCNA that facilitates its degradation. This PCNA-mediated protein degradation pathway has been well established for several other PCNA-interacting proteins including the cyclin-dependent protein kinase inhibitor p21, the DNA licensing factor Cdt1, and DNA polymerase η (Soria and Gottifredi, 2010). After their initial functions in preparing the cell for DNA replication, p21 and Cdt1 are degraded through their interaction with PCNA as their continued activity would thwart the streamlined and productive process of DNA replication. In the case of DNA polymerase η, interaction with PCNA results in its subsequent degradation presumably as a means to switch to the next appropriate DNA polymerase (Soria and Gottifredi, 2010). Our results show that PR-Set7 facilitates 53BP1 recruitment to DNA damage foci and is then similarly subjected to PCNA-mediated degradation. Moreover, this degradation pathway dictates the strict regulation of PR-Set7 during the cell cycle.

Results

PR-Set7 is Undetectable in S Phase

In order to scrutinize the reported PR-Set7 function during S phase, especially in light of its interaction with PCNA, we devised an assay to quantify PR-Set7 during the cell cycle. We generated a U2OS human osteosarcoma cell line that expresses a stably transfected enhanced yellow fluorescent protein (YFP)-tagged PR-Set7. We performed FACS analyses to examine the expression of YFP-PR-Set7 during the cell cycle. Interestingly, only ~23% of cells stably transfected and selected to express YFP-PR-Set7 were YFP-positive (Figure1A, top panel). This was the case even after two rounds of FACS sorting the cells to near 100% homogeneity. A closer analysis of the FACS data revealed that of the YFP-positive cells (24% of the total population), 38% are in G1, 55% are in G2/M, and only 7% are in S (Figure 1A, top panel). To verify that the fluorescence signal obtained was solely reflective of PR-Set7 levels, we performed the experiment using two siRNAs specific to PR-Set7, along with a control siRNA against GADPH (Figure 1A, bottom panels). As expected, both siRNAs specific to PR-Set7 resulted in markedly reduced levels of fluorescence while siRNA-GADPH was ineffectual.

To ascertain the presence of YFP-PR-Set7 throughout the cell cycle, we employed single-cell time-lapse imaging. In this case, we also compared the protein levels of transiently transfected mCherry-tagged proliferating cell nuclear antigen (PCNA) (mCherry-PCNA) (Figure 1B). While PCNA is clearly visible during each phase of the cell cycle tested, PR-Set7 was not detectable at any time during S-phase (Figure 1Ba-c and n). PR-Set7 remains undetectable in early G2 (Fig. 1Bd), and becomes visible in a diffuse nuclear pattern in late G2 about 2h before mitosis (Figure1Be-f). During chromatin condensation in prophase, PR-Set7 assumes a more uneven distribution (Figure 1Bg), in accordance with its binding to chromosomes as shown previously (Rice et al., 2002). During mitosis, PR-Set7 remains associated with chromosomes (Figure 1Bh-i) and segregates with the chromatids to the daughter nuclei (Figure 1Bj). Upon chromosome decondensation in early G1, PR-Set7 again assumes a diffuse localization and its levels decrease to being almost undetectable within about 4h after cell division (Figure 1Bk-l). PR-Set7 then remains undetectable for the remainder of G1 and throughout the next S-phase (Figure 1Bm-n). Given these results, along with the FACS analyses shown above, and our previous findings (Oda et al., 2009), we conclude that PR-Set7 is absent during S-phase.

Functional Characterization of the PR-Set7 PIP Domains

Since PR-Set7 was undetectable in S-phase, we next sought to understand the biological relevance of its reported interaction with PCNA (Huen et al., 2008; Jorgensen et al., 2007; Warbrick, 1998). We first analyzed whether each of the previously mapped PIP domains within PR-Set7 is responsible for its interaction with PCNA. Figure 1C shows a schematic representation of the defined domains of note within PR-Set7 including SET, PIP1, and PIP2. Based on the PIP domain residues that were shown to be important for interaction with PCNA (Huen et al., 2008; Jorgensen et al., 2007), we derived mutations in either PIP1 (m1) or PIP2 (m2) or both (m1/m2). Using recombinant FLAG-tagged PR-Set7 and PCNA, their interaction was evident in FLAG-immunoprecipitations only when both PIP domains were intact (Figure 1D). A double mutant m1/m2, as well as the PIP2 mutant did not show any binding affinity to PCNA, while a mutation in the PIP1 domain retained some residual PCNA binding (Figure 1D).

We next tested if the PIP domains within PR-Set7 that are required for its interaction with PCNA could exhibit a functional consequence to a well-documented PCNA-dependent process, that of DNA synthesis. DNA synthesis by DNA polymerase δ was scored *in vitro*

using a primed single-stranded DNA template in the presence of radiolabelled dCTP and as a function of the presence of increasing amounts of PCNA (Figure 1E). As expected, PCNA was required for DNA polymerization (lanes 4-7) and the reaction was saturated at the second incremental amount of PCNA added. Previous studies elucidated that the p21-mediated inhibitory effect on DNA synthesis was due to the PIP domain-dependent interaction of p21 with PCNA (Gibbs et al., 1997). This p21 inhibitory effect was reproduced in the assay shown (lanes 8-10), and was reversed by the addition of higher PCNA levels (lane 10). Similar to the case of p21, the addition of PR-Set7 resulted in inhibition of DNA synthesis that was overcome only in the presence of elevated PCNA levels (lanes 11-13). Moreover, the PIP domains of PR-Set7 were required for its inhibitory effect, as the m1/m2 mutant of PR-Set7 was ineffectual (lanes 14-16). The quantification of these results are shown in Figure 1E and indicate that the interaction of PCNA and PR-Set7 mediated through its PIP domains stably sequester PCNA.

PCNA Recruits PR-SET7 to DNA Damage Sites

PCNA has a role not only in DNA replication, but also in DNA damage repair (Essers et al., 2005; Moldovan et al., 2007; Solomon et al., 2004). Given the interaction of PR-Set7 with PCNA, we hypothesized that PR-Set7 might function in DNA repair. To test this hypothesis, we induced DNA double strand breaks by a localized irradiation (405nm laser) of Hoechst sensitized U2OS cells expressing YFP-PR-Set7 (Figure 2A). DNA double-strand breaks were scored by the appearance of immunofluorescently labelled γ-H2A.X at the irradiation site (Figure 2A). Importantly, YFP-PR-Set7 co-localizes with γ-H2A.X, indicating that PR-Set7 accumulates at sites of DNA damage (Figure 2A). Similarly, U2OS cells stably expressing reciprocally tagged proteins, YFP-PCNA and mCherry-PR-Set7 exhibited co-localization of PCNA and PR-Set7 at the site of laser-induced DNA damage (Figure 2B).

We next examined as a function of time, the appearance of PCNA and of PR-Set7 at the site of laser-induced DNA damage using time-lapse microscopy (Figure 2B). PCNA was detectable at the damage site very rapidly (within 6 sec), while PR-Set7 recruitment is delayed (12 sec) (Figure 2E). This result suggested the possibility that PCNA interaction with PR-Set7 might recruit PR-Set7 to the damage site and, if this were to be the case, the PR-Set7 domains requisite for such interaction would be expected to be required for its recruitment. Indeed, a similar analysis performed with U2OS cells stably expressing YFP-PCNA and this time with a mCherry-tagged PR-Set7 PIP domains mutant (mCherry-PR-Set7-m1/m2) showed a similar profile for PCNA recruitment at the DNA damage site, indicating that PCNA recruitment is independent of interaction with PR-Set7 (Figure 2C). Conversely, PR-Set7-m1/m2 mutant was not recruited, demonstrating that the PR-Set7 PIP domains are essential for its binding to DNA double strand breaks (Figure 2C). This was not the case however with the SET domain mutant of PR-Set7 (R265G) that was recruited similarly to the case of wild-type PR-Set7 (Figure 2D). These results indicate that PCNA recruits PR-Set7 to sites of DNA damage through its direct interaction with the PR-Set7 PIP domains.

Active PR-Set7 Recruits 53BP1 to DNA Damage Sites

The results described above demonstrate that PR-Set7 is transiently recruited to the DNA damage site through its interaction with PCNA, suggesting that PR-Set7 might play a role in this process. We first sought to identify cellular proteins interacting with the product of PR-Set7 catalysis, H4K20me1 using a SILAC-based histone peptide pull-down approach (Vermeulen et al., 2007). The analysis shows that the protein that displayed significant H4K20me1 binding in this assay was 53BP1 (Figure 3A). 53BP1 is a key regulator of the DNA damage checkpoint response (FitzGerald et al., 2009) and was previously reported to target H4K20me1-2 for binding (Botuyan et al., 2006; Sanders et al., 2004). As a control, we

also evaluated binding proteins for H4K20me2 and found that although 53BP1 recognized this modification also, it is no longer the most enriched protein as it was in the case of H4K20me1 (Figure 3B). (For comparison of the proteins bound to H4K20me1 and H4K20me2, see Supplementary Tables 1 and 2). We next tested if PCNA-mediated recruitment of PR-Set7 may impact the appearance of 53BP1 at laser-induced DNA damage sites.

Both PR-Set7 and 53BP1 were indeed recruited to the site of laser-induced DNA damage in cells expressing YFP-PR-Set7 and mCherry-53BP1, and the appearance of PR-Set7 preceded that of 53BP1 (Figure 3C). This suggested that PR-Set7-mediated catalysis of H4K20me1 might provide the necessary target for 53BP1 recruitment to the site of DNA damage. To test this hypothesis, we first established conditions to eliminate participation by endogenous PR-Set7. Knockdown of endogenous PR-Set7 was achieved through specific RNAi treatment for a period of three days (see Figures 1A and 3F for knockdown of PR-Set7). These cells were then transfected with a plasmid expressing mCherry-53BP1. Importantly, knockdown of PR-Set7 prevents the recruitment of 53BP1 to a DNA damage site (Figure 3F). This indicates that 53BP1 recruitment depends on PR-Set7. To test if PR-Set7 catalytic activity is necessary for 53BP1 recruitment, we rescued the PR-Set7 knockdown cells with siRNA resistant YFP-PR-Set7 (WT, Figure 3D) or YFP-PR-Set7 mutant in its catalytic domain (R265G, Figure 3E), and co-transfected mCherry-53BP1. Both wt PR-Set7 and 53BP1 were recruited to the DNA damage site with 53BP1 appearing after PR-Set7, as expected, based on the results shown above (Figure 3C). However, while the PR-Set7 mutant in its catalytic domain was recruited, 53BP1 recruitment was undetectable (Figure 3E). This result strongly suggests that PR-Set7-mediated *de novo* mono-methylation of H4K20 is required to recruit 53BP1 to the site of DNA damage. We extended the results discussed above and analyzed whether the recruitment of endogenous 53BP1 to DNA damage sites was dependent on PR-Set7 and found this to be the case (Figure 3G).

PR-Set7 is Unstable after DNA-Damage is Incurred

That PR-Set7 was recruited to sites of DNA damage was unexpected and undoubtedly a key aspect of its functional role and/or regulation. Given that our results demonstrated that PR-Set7 is absent in S-phase and that its occupancy at a DNA damage site is transient (data not shown), we next examined if PR-Set7 was regulated post-transcriptionally. We first gauged PR-Set7 levels as a function of cellular exposure to DNA damaging agents. U2OS cells were subjected to a panel of different DNA damaging agents including UV, methylmethane sulfate (MMS), hydroxyurea (HU), hydrogen peroxide, and adriamycin. DNA damage occurred in these cases as evidenced by the increased levels of Chk1 that was phosphorylated at serine 317 (Figure 4A). Quite remarkably, PR-Set7 levels were decreased relative to those of PCNA in the case of all DNA damaging agents tested, with UV treatment causing the largest effect (PR-Set7 degradation as a function of UV dose is shown in Supplementary Figure 1). To further investigate the regulation of PR-Set7 protein levels, HEK293T cells were subjected to UV irradiation and the levels of PR-Set7 and PCNA were gauged as a function of time post-treatment using western blot analysis (Figure 4B). In contrast to PCNA, the levels of which appeared stable throughout the times tested, PR-Set7 levels declined steadily such that the protein was barely detectable at 4 hours post-UV treatment (Figure 4B). To determine if PR-Set7 was being subjected to degradation, we compared its levels in the absence and presence of two different inhibitors of protein degradation, the proteasome inhibitor MG132 and the E1 ubiquitin activating enzyme inhibitor UBEI-41. Western blot analyses demonstrated that the loss of PR-Set7 upon UV irradiation was prevented by either of those two inhibitors (Figure 4C). This result indicates that PR-Set7 is targeted for proteasomal degradation upon UV-induced DNA damage.

PR-Set7 is Degraded via the PCNA-Activated Ubiquitin Proteasome Pathway

Our finding that PR-Set7 is regulated at the post-translational level upon cellular exposure to DNA damaging agents was of prime interest given its absence during DNA replication in S-phase, and its interaction via its PIP domains with PCNA that functions at chromatin during DNA repair. Several reports have documented that chromatin bound PCNA can promote ubiquitin-coupled, proteasome-mediated degradation of its interacting partners whose continued function would be detrimental to the cell (Soria and Gottifredi, 2010). Two such cases involve the cyclin-dependent kinase inhibitor p21 (Abbas et al., 2008; Kim et al., 2008; Nishitani et al., 2008) and the DNA licensing factor Cdt1 (Arias and Walter, 2006; Nishitani et al., 2006; Senga et al., 2006) that are subjected to degradation by the $CRL4^{Cdt2}$ E3 ligase as a function of their interaction with chromatin-bound PCNA through their respective PIP domains. The PIP2 domain of PR-Set7 shares the reported features of the specialized PIP sequence on p21 or Cdt1, which are TD residues at positions 5 and 6 of the PIP box and a basic residue at +4 (Figure 4D) (Havens and Walter, 2009). Indeed, UV-treatment of cells containing the m1 mutant of PR-Set7 demonstrated that the protein was degraded to an extent similar to that of wild-type PR-Set7, while the m2 and the m1/m2 mutants of PR-Set7 were resistant to this process, as shown by western blot analyses (Figure 4E). Moreover, in the case of untreated cells, the basal levels of m2 and m1/m2 mutant proteins were markedly elevated in comparison to those of either wild type or m1 mutant PR-Set7 (Figure 4E).

In order to determine if PCNA binding is essential for PR-Set7 degradation, we employed the well established interaction of p21 with PCNA. Wild-type p21 competitively binds to PCNA, which prevents UV-induced PR-Set7 degradation (Figure 4F). Conversely, a p21 PIP mutant devoid in PCNA binding does not prevent PR-Set7 degradation (Figure 4F). The inhibition of PR-Set7 degradation by p21 can be negated by excess YFP-PCNA. These data show that the direct interaction with PCNA is essential for PR-Set7 degradation.

Given that UV-induced PR-Set7 degradation requires the direct interaction with PCNA, we tested if this interaction is also required for PR-Set7 degradation during the cell cycle. FACS analyses demonstrated that HEK293T cells expressing PR-Set7, either wt or mutant in its PIP1 domain (m1) or in its SET domain (R265G), exhibited undetectable levels during S-phase, whether treated with UV or not (Figure 4G). In contrast, the cells expressing the PIP2 mutant of PR-Set7 (m2 or m1/m2) gave rise to clearly detectable levels of PR-Set7 protein in S-phase, irrespective of UV treatment (Figure 4G). These results strongly suggest that the direct interaction of PR-Set7 with PCNA through its PIP2 domain targets PR-Set7 for degradation by the ubiquitin-proteasome pathway during the cell cycle and during DNA repair. Consistent with these findings, U2OS cells expressing mCherry-PCNA and YFP-PR-Set7-m2 exhibit diffuse and clearly detectable PR-Set7 in the nucleus during all S-phase stages, as evidenced by live cell imaging analysis (data not shown).

Two Independent Pathways Operate to Regulate PR-Set7 Stability

Skp2 was previously shown to target PR-Set7 for proteasomal degradation (Yin et al., 2008). To evaluate the role of Skp2 in the destabilization of PR-Set7, *Skp2*$^{-/-}$ and WT MEFs were subjected to UV treatment. PR-Set7 was completely stabilized in whole cell extracts after UV treatment in the *Skp2*$^{-/-}$ MEFs relative to WT (Figure 5A, left panel), yet this stabilization was markedly decreased in the chromatin bound fraction (Figure 5A, right panel). Thus Skp2 regulates PR-Set7 levels predominantly outside the context of chromatin.

The CRL4/Cdt2-mediated degradation of PCNA-interacting proteins such as p21 and Cdt1, as well as DNA polymerase η, and E2F occurs during S-phase and during the incurrence of DNA-damage, and is chromatin-localized (Soria and Gottifredi, 2010). The specificity

inherent to this process depends on Cdt2 that functions as the substrate receptor and recruits a particular targeted protein to the E3 ubiquitin ligase module containing Cul4 and DDB1. Given our results that p21 over-expression inhibited PR-Set7 degradation, we first tested if, similar to p21 and the other documented PCNA targets, PR-Set7 degradation also relies on Cdt2. HEK293T cells were treated with either siRNA specific to DDB1 or a control siRNA and the levels of PR-Set7 after UV irradiation were gauged by western blot (Figure 5B). Decreased levels of DDB1 correlated with increased levels of PR-Set7, suggesting that DDB1 is likely involved in PR-Set7 degradation. Similar results were obtained upon decreasing the levels of Cdt2 (Figure 5C), suggesting that Cdt2 is likely the receptor in PR-Set7-mediated degradation. Consistent with this, over-expression of FLAG-tagged Cdt2 resulted in lower levels of PR-Set7, relative to the empty vector control (Figure 5D). Importantly, the steady state levels of PR-Set7 were higher upon DDB1 and Cdt2 depletion, yet PR-Set7 was still degraded, suggesting that other E3 ligase(s) also contribute to PR-Set7 stability, consistent with the findings presented above that Skp2 also regulates PR-Set7 levels.

To ascertain if PR-Set7 can be ubiquitylated *in vivo*, we performed transfections of HA-ubiquitin in HEK293T cells, in the absence and presence of MG132 treatment. Western blot analysis of immunoprecipitated, endogenous PR-Set7 performed using anti-HA antibody revealed PR-Set7 *in vivo* polyubiquitylation after addition of MG132 (Figure 5E). To determine whether the $CRL4^{Cdt2}$ E3 ligase complex can directly promote ubiquitylation, we performed ubiquitylation assays *in vitro* using affinity purified $CRL4^{Cdt2}$ complex from HEK293T cells (Figure 5F). Indeed, PR-Set7 was ubiquitylated (Ub-PR-Set7) dependent on the presence of the E2 enzyme and the E3 ligase CRL4/Cdt2, (Figure 5F). Moreover, the conditions of the assay were in the linear range, as increased levels of Ub-PR-Set7 were achieved upon the addition of an increasing amount of the $CRL4^{Cdt2}$ complex. These results demonstrate that PR-Set7 is directly ubiquitylated by the $CRL4^{Cdt2}$ complex. This Cdt2-dependent ubiquitylation of PR-Set7 accounts for the inverse correlation of PR-Set7 and Cdt2 levels observed upon manipulation of Cdt2 levels *in vivo* (Figure 5D). We conclude that PR-Set7 degradation upon DNA damage repair involves its PIP2 domain-mediated interaction with PCNA, which leads to its polyubiquitylation by $CRL4^{Cdt2}$ and subsequent proteasomal degradation.

Discussion

Our findings demonstrate two functional outcomes to PR-Set7 interaction with PCNA that impact appropriate cellular functioning and viability. PCNA recruits PR-Set7 to sites of DNA damage where an active PR-Set7 is required to recruit 53BP1 that galvanizes the cellular response to DNA damage. The second outcome of PCNA interaction with, and recruitment of PR-Set7 to DNA, results in its degradation. PCNA-mediated degradation of PR-Set7 limits its presence after DNA damage occurs and stringently controls its presence during the cell cycle. PR-Set7 can now be considered a member of a class of proteins, including p21 and Cdt1, whose continued activity would jeopardize and interfere with the appropriate progression of DNA replication and/or genomic integrity. Consequently, the cell evolved a mechanism to target these activities for elimination through interaction with PCNA at the site of their functioning, the chromatin milieu. Through its PIP2 domain, a region highly homologous with the PIP domains of p21 and Cdt1, PR-Set7 is sequestered by PCNA and subjected to PCNA-mediated degradation. As in these other cases, PR-Set7 is polyubiquitylated by the $CRL4^{Cdt2}$ ubiquitin ligase and subsequently degraded by the proteasome. However, it is important to stress that other degradation pathways also operate in regulating the cellular concentration of PR-Set7 as previous studies documented, and our work shows that Skp2 regulates PR-Set7 (Yin Y et. al. 2008). This would be consistent with our findings demonstrating that upon decreasing the intracellular levels of Cdt2, the steady-

state levels of PR-Set7 were increased, yet PR-Set7 was still subjected to degradation (Figure 5).

Temporal Regulation of PR-Set7 via PCNA Interaction

Previous studies reported the co-localization of PR-Set7 and PCNA during S phase, and that PR-Set7 contains PIP domains required for this co-localization (Huen et al., 2008; Jorgensen et al., 2007; Tardat et al., 2007). These studies suggested a functional role for PR-Set7 in DNA replication during S phase. Of note, PR-Set7 was detected at PCNA foci only in the presence of proteasome inhibitor during S phase. Another report showed that over-expressed PR-Set7 was present in the cytoplasm using live cell imaging (Yin et al., 2008). Our data confirm the existence of two PIP domains within PR-Set7 and that each bind to PCNA *in vitro*. However, we do not detect PR-Set7 under physiological conditions during S phase either in the nucleus or the cytoplasm. Instead, we detect PR-Set7 protein from late G2 through mitosis until early G1 phases. These findings are consistent with our previous report that demonstrated the absence of PR-Set7 during S-phase using synchronized cells (Oda et al., 2009). Given that PR-Set7 is the sole methyltransferase responsible for H4K20 monomethylation, our previous studies also indicated that the temporal change in PR-Set7 levels during the cell cycle was reflected by increased levels of H4K20me1 at late G2 and decreased levels in G1-S (Oda et al., 2009). In the present studies, we demonstrate the mechanism by which PR-Set7 is absent during DNA replication.

Although YFP-PR-Set7 expression at the transcriptional level is driven by a constitutive promoter in the stable cell lines used herein, and its expression at the protein level exceeded that of endogenous PR-Set7 in asynchronized cells both endogenous PR-Set7 and exogenous, tagged PR-Set7 exhibited similar temporal expression as a function of the cell-cycle. This is consistent with PR-Set7 expression being controlled mainly through post-translational modification(s) such as ubiquitylation.

$CRL4^{Cdt2}$ Target PR-Set7 for Degradation

A previous study reported SCF/Skp2 to be an E3 ligase for PR-Set7 (Yin et al., 2008). Here, we identified $CRL4^{Cdt2}$ as a novel E3 ubiquitin ligase for PR-Set7. The $CRL4^{Cdt2}$ complex targets various proteins such as p21 (Abbas et al., 2008; Kim et al., 2008; Nishitani et al., 2008), Cdt1 (Nishitani et al., 2006), DNA Polymerase η (Kim and Michael, 2008), and E2F (Shibutani et al., 2008) through their individual interaction with PCNA. The interaction of PR-Set7 with PCNA is essential for the recruitment of the $CRL4^{Cdt2}$ E3 complex. This interaction is dependent on the presence of a specialized PIP box called the “PIP degron” in each targeted protein. The introduction of a mutation within the PR-Set7 PIP2 site inhibited its interaction with PCNA and its degradation during the cell cycle and after UV irradiation. Therefore this E3 ubiquitin ligase system is a major post-translational mechanism regulating PR-Set7 levels. Another important feature of this degradation pathway is that it is activated only when PCNA is bound to chromatin, thereby limiting its effectiveness to the periods of time when the cell replicates its DNA or incurs DNA damage (Arias and Walter, 2006; Havens and Walter, 2009).

Functional Significance of Undetectable PR-Set7 During S Phase

Why is PR-Set7 degraded prior to S phase? Along with PR-Set7, H4K20 methylation also changes dynamically during the cell cycle (Oda et al., 2009). Newly deposited histone H4 during S phase is not methylated at H4K20. Monomethylation at K20 is strictly nucleosomal dependent (Nishioka et al., 2002) and begins at G2 when PR-Set7 is present (Rice et al., 2002); (Oda et al., 2009). During the following mitotic and G1 phases, H4K20me1 is converted to H4K20me2 and H4K20me3 by the enzymatic activity of the Suv4-20s (Pesavento et al., 2008). Bolstering that this sequential methylation of H4K20 occurs *in vivo*

is the finding that Suv4-20h1 and Suv4-20h2 double knockout cells accumulate elevated amounts of H4K20me1, but lack H4K20me2 and -me3 (Schotta et al., 2008). This sequential methylation during the cell cycle is tightly regulated by the temporal expression of the responsible enzymes.

In our previous studies using conditional PR-Set7 knockout ES cells, these deficient cells were able to exhibit a seemingly normal mitotic phase even though it is during this period that H4K20me1 would normally reach its peak level during the cell cycle. Instead, PR-Set7 knockout cells arrested at the first S phase in the resultant daughter cells (Oda et al., 2009). Other reports also documented an S phase delay due to PR-Set7 knockdown (Jorgensen et al., 2007; Tardat et al., 2007). These reports suggested that the speed of the replication fork was slowed and hypothesized that PR-Set7 has substrate(s) other than histone H4 during S phase to promote S phase progression (Tardat et al., 2007). Nevertheless, our previous results, confirmed by our results here, show that PR-Set7 is undetectable during S phase, under physiological conditions. Thus, we infer that PR-Set7 cannot play a direct role during replicative DNA synthesis. Instead, we hypothesize that the decreased level of methylated H4K20 or increased level of unmethylated H4K20 causes disturbed S phase progression in the daughter cells that were derived from parental cells lacking PR-Set7 in the preceding cell cycle.

The results presented herein are summarized in Figure 6 and establish an important role for PR-Set7 in maintaining genome integrity. It is not unexpected that an enzyme whose product is important for chromosome condensation (Oda et al., 2009) is tightly regulated during the cell cycle. The absence of PR-Set7 in the S-phase of the cell cycle allows for the dilution of the H4K20me1 mark and likely appropriate DNA replication. H4K20me1 is re-established during mitosis prior to chromosome condensation and segregation. Of note, most of the dynamic alterations in chromosome structure appear to be regulated by the H4 tail. Acetylation at lysine-16 is required to establish an open chromatin structure (Shogren-Knaak et al., 2006) whereas monomethylation at lysine-20 is required for appropriate chromosome compaction. Most likely the placement of these two modifications are highly regulated and mutually exclusive or one modification may silence the other one. Additionally, the H4K20 residue appears to be critical in DNA repair. H4K20me1 not only provides a recruitment site for 53BP1 as demonstrated in the studies presented herein, but also provides the substrate for the action of the Suv4-20 enzymes that catalyze H4K20me2-3, a modification also involved in formation of high order chromatin structures and in DNA damage repair (Schotta et al., 2008).

Experimental Procedures

FACS analysis

Cells were fixed with 70% ethanol and stained with propidium iodide and analyzed using the LSRII (Becton Dickinson) flow cytometer.

Cell culture

HEK 293 and U2OS cells were grown according to standard procedures. Stable cell lines expressing PR-Set7 or PCNA were derived after transfection by electroporation with 2 μg of plasmid expressing EYFP-PR-Set7 or pEYFP-PCNA, followed by selection with G418 for 2 weeks, and then FACS sorting for equal expression levels. For cell lines stably expressing both PR-Set7 and PCNA, U2OS EYFP-PCNA cells were transduced with retrovirus obtained using the pMSCV-EYFP-PR-Set7 plasmid and selected with 1 mg/ml Puromycin for 1 week. Transient transfections of U2OS cells were performed by electroporation using 2 μg of plasmid, then plated on MatTek glass bottom dishes (Mattek, Corp, Ashland, MA),

and data acquistion started 24 h post-transfection. For UV-induced DNA damage experiments, HEK293T cells treated with 400 J/m^2 UV were harvested and extracts prepared as described previously (Oda et al., 2009).

Live cell microscopy and laser irradiation

For long-term live cell imaging, cells were kept in DMEM supplemented with 20% FCS in an environmental chamber equilibrated at 37°C and 5% CO_2. Image acquisition was performed on an Applied Precision Deltavision Core microscope (Applied Precision, Issaquah, WA). Image stacks (20×1 μm, 2×2 binning) were recorded every 20 min, deconvolved and subjected to maximum intensity projection. Exposure times were kept to a minimum to minimize photobleaching; UV wavelengths were filtered out where applicable. For laser irradiation experiments, cells were sensitized with 0.2 μg/ml Hoechst33342 for 20 min in DMEM supplemented with 10% FCS, washed, and the medium was replaced with phenol red-free DMEM supplemented with 20% FCS. Individual cells were irradiated with a 1 sec pulse at 100% power of a 10mW 405nM solid state laser on the Deltavision Core microscope. Data acquisition was started immediately after the laser pulse, and 8×1 μm image stacks (2×2 binning) were recorded every 6 sec. Images were subjected to maximum intensity projection, and quantifications were performed using the SoftWorx program and standard office software. Immunofluorescence labeling was performed according to standard procedures using 5 μg/ml anti-Phospho-H2A.X antibody (ThemoScientific, MA) at 4°C overnight, followed by TexasRed coupled anti-mouse secondary antibody (1 h, room temperature).

Histone peptide pull-downs and mass spectrometry

SILAC labeled HeLa chromatin pellets obtained after nuclear extraction according to Dignam et al. (Dignam et al., 1983) were resolubilized in 150 mM NaCl, 50 mM Tris, 1% NP40 and 5 mM $MgCl_2$ in the presence of Benzonase (Merck) at roomtemperature in a thermoshaker. Following centrifugation, solubilized proteins were aliquoted, snap-frozen after addition of 10% v/v glycerol and stored at -80°C until further usage. Unmodified or H4K20me1 containing H4 peptides covering amino acids 12-27 and carrying a biotinylated lysine residue on the C-terminus were synthesized as described (Vermeulen et al., 2007). Lyophilized peptides were dissolved in a Tris buffered solution and immobilized on Dynabeads M280 Streptavidin (Invitrogen) equilibrated in binding buffer (150 mM NaCl, 50 mM Tris-HCl pH 8.0, 0.25% NP40, 0.5 mM DTT and complete protease inhibitors −EDTA (Roche)). Beads were then incubated with 500 micrograms of SILAC labeled resolubilized nuclear pellets diluted to a final concentration of 0.8 mg/ml in binding buffer for 4 h at 4°C. Beads were washed extensively in binding buffer after which bound proteins were eluted in SDS PAGE loading buffer and subjected to in-gel trypsin digestion as described (Vermeulen et al., 2007). Gel lanes of each pull-down were cut into eight slices which were independently further sliced into smaller pieces. Peptide extraction was performed as described (Vermeulen et al., 2007). Peptide identification experiments were performed using an EASY-nLC system from Proxeon connected online to an LTQ-Orbitrap-Velos mass spectrometer (Thermo Scientific, Germany). Tryptic peptides were separated according to their hydrophobicity using a 5-30% acetonitrile gradient on a 15 cm reverse phase column with an inner diameter of 75 um packed with C18 material (Dr. Maisch). The mass spectrometer was operated in the data-dependent mode to switch between MS and MS/MS. Full scan MS spectra were acquired with a resolution of 60,000 and for every full scan the 15 most intense ions were fragmented in the dual pressure linear ion trap. Raw data was processed and analyzed using Maxquant software version 1.0.13.12 and searched with the Mascot search engine against human IPI database 3.52.

Supplementary Material

Refer to Web version on PubMed Central for supplementary material.

Acknowledgments

We are grateful to Stephanie Kim, Deborah Hernandez, Kettly Cabane, and Jingjing Li for technical assistance and members of the Reinberg lab for helpful discussions. We also thank Kathleen Gildea and Kamilah Ryan for assistance with FACS analysis; Keiko Nakayama for the *Skp2*-/- MEFs, Anindya Dutta for the Cul4, DDB1, Cdt2 and Rbx1 expression plasmids, Titia de Lange for the pmCherry-53BP1 plasmid, Hideo Nishitani for the p3xFlag-p21 plasmid; Roberto Bonasio, Tony Huang, Luca Colnaghi, and Mathew Jones for experimental advice, and Lynne Vales for comments on the manuscript. This work was supported by grants from NIH GM64844 (to D.R.), and the HHMI (to D.R.). Research in the Spector laboratory is funded by NIH GM42694. M.R.H. was supported by fellowships from European Molecular Biology Organization (EMBO; ALTF 160-2005) and the German Academic Exchange Service (DAAD).

References

Abbas T, Sivaprasad U, Terai K, Amador V, Pagano M, Dutta A. PCNA-dependent regulation of p21 ubiquitylation and degradation via the CRL4Cdt2 ubiquitin ligase complex. Genes Dev 2008;22:2496–2506. [PubMed: 18794347]

Anastassiadis K, Kim J, Daigle N, Sprengel R, Scholer HR, Stewart AF. A predictable ligand regulated expression strategy for stably integrated transgenes in mammalian cells in culture. Gene 2002;298:159–172. [PubMed: 12426104]

Arias EE, Walter JC. PCNA functions as a molecular platform to trigger Cdt1 destruction and prevent re-replication. Nat Cell Biol 2006;8:84–90. [PubMed: 16362051]

Botuyan MV, Lee J, Ward IM, Kim JE, Thompson JR, Chen J, Mer G. Structural basis for the methylation state-specific recognition of histone H4-K20 by 53BP1 and Crb2 in DNA repair. Cell 2006;127:1361–1373. [PubMed: 17190600]

Dignam JD, Lebovitz RM, Roeder RG. Accurate transcription initiation by RNA polymerase II in a soluble extract from isolated mammalian nuclei. Nucleic Acids Res 1983;11:1475–1489. [PubMed: 6828386]

Essers J, Theil AF, Baldeyron C, van Cappellen WA, Houtsmuller AB, Kanaar R, Vermeulen W. Nuclear dynamics of PCNA in DNA replication and repair. Mol Cell Biol 2005;25:9350–9359. [PubMed: 16227586]

FitzGerald JE, Grenon M, Lowndes NF. 53BP1: function and mechanisms of focal recruitment. Biochem Soc Trans 2009;37:897–904. [PubMed: 19614615]

Gibbs E, Kelman Z, Gulbis JM, O'Donnell M, Kuriyan J, Burgers PM, Hurwitz J. The influence of the proliferating cell nuclear antigen-interacting domain of p21(CIP1) on DNA synthesis catalyzed by the human and Saccharomyces cerevisiae polymerase delta holoenzymes. J Biol Chem 1997;272:2373–2381. [PubMed: 8999948]

Havens CG, Walter JC. Docking of a specialized PIP Box onto chromatin-bound PCNA creates a degron for the ubiquitin ligase CRL4Cdt2. Mol Cell 2009;35:93–104. [PubMed: 19595719]

Huen MS, Sy SM, van Deursen JM, Chen J. Direct interaction between SET8 and proliferating cell nuclear antigen couples H4-K20 methylation with DNA replication. J Biol Chem 2008;283:11073–11077. [PubMed: 18319261]

Jorgensen S, Elvers I, Trelle MB, Menzel T, Eskildsen M, Jensen ON, Helleday T, Helin K, Sorensen CS. The histone methyltransferase SET8 is required for S-phase progression. J Cell Biol 2007;179:1337–1345. [PubMed: 18166648]

Kim SH, Michael WM. Regulated proteolysis of DNA polymerase eta during the DNA-damage response in C. elegans. Mol Cell 2008;32:757–766. [PubMed: 19111656]

Kim Y, Starostina NG, Kipreos ET. The CRL4Cdt2 ubiquitin ligase targets the degradation of p21Cip1 to control replication licensing. Genes Dev 2008;22:2507–2519. [PubMed: 18794348]

Kouzarides T. Chromatin modifications and their function. Cell 2007;128:693–705. [PubMed: 17320507]

Li B, Carey M, Workman JL. The role of chromatin during transcription. Cell 2007;128:707–719. [PubMed: 17320508]

Margueron R, Trojer P, Reinberg D. The key to development: interpreting the histone code? Curr Opin Genet Dev 2005;15:163–176. [PubMed: 15797199]

Moldovan GL, Pfander B, Jentsch S. PCNA, the maestro of the replication fork. Cell 2007;129:665–679. [PubMed: 17512402]

Nishioka K, Rice JC, Sarma K, Erdjument-Bromage H, Werner J, Wang Y, Chuikov S, Valenzuela P, Tempst P, Steward R, et al. PR-Set7 is a nucleosome-specific methyltransferase that modifies lysine 20 of histone H4 and is associated with silent chromatin. Mol Cell 2002;9:1201–1213. [PubMed: 12086618]

Nishitani H, Shiomi Y, Iida H, Michishita M, Takami T, Tsurimoto T. CDK inhibitor p21 is degraded by a proliferating cell nuclear antigen-coupled Cul4-DDB1Cdt2 pathway during S phase and after UV irradiation. J Biol Chem 2008;283:29045–29052. [PubMed: 18703516]

Nishitani H, Sugimoto N, Roukos V, Nakanishi Y, Saijo M, Obuse C, Tsurimoto T, Nakayama KI, Nakayama K, Fujita M, et al. Two E3 ubiquitin ligases, SCF-Skp2 and DDB1-Cul4, target human Cdt1 for proteolysis. EMBO J 2006;25:1126–1136. [PubMed: 16482215]

Oda H, Okamoto I, Murphy N, Chu J, Price SM, Shen MM, Torres-Padilla ME, Heard E, Reinberg D. Monomethylation of histone H4-lysine 20 is involved in chromosome structure and stability and is essential for mouse development. Mol Cell Biol 2009;29:2278–2295. [PubMed: 19223465]

Pesavento JJ, Yang H, Kelleher NL, Mizzen CA. Certain and progressive methylation of histone H4 at lysine 20 during the cell cycle. Mol Cell Biol 2008;28:468–486. [PubMed: 17967882]

Rice JC, Nishioka K, Sarma K, Steward R, Reinberg D, Allis CD. Mitotic-specific methylation of histone H4 Lys 20 follows increased PR-Set7 expression and its localization to mitotic chromosomes. Genes Dev 2002;16:2225–2230. [PubMed: 12208845]

Sanders SL, Portoso M, Mata J, Bahler J, Allshire RC, Kouzarides T. Methylation of histone H4 lysine 20 controls recruitment of Crb2 to sites of DNA damage. Cell 2004;119:603–614. [PubMed: 15550243]

Schotta G, Sengupta R, Kubicek S, Malin S, Kauer M, Callen E, Celeste A, Pagani M, Opravil S, De La Rosa-Velazquez IA, et al. A chromatin-wide transition to H4K20 monomethylation impairs genome integrity and programmed DNA rearrangements in the mouse. Genes Dev 2008;22:2048–2061. [PubMed: 18676810]

Senga T, Sivaprasad U, Zhu W, Park JH, Arias EE, Walter JC, Dutta A. PCNA is a cofactor for Cdt1 degradation by CUL4/DDB1-mediated N-terminal ubiquitination. J Biol Chem 2006;281:6246–6252. [PubMed: 16407252]

Shi X, Kachirskaia I, Yamaguchi H, West LE, Wen H, Wang EW, Dutta S, Appella E, Gozani O. Modulation of p53 function by SET8-mediated methylation at lysine 382. Mol Cell 2007;27:636–646. [PubMed: 17707234]

Shibutani ST, de la Cruz AF, Tran V, Turbyfill WJ 3rd, Reis T, Edgar BA, Duronio RJ. Intrinsic negative cell cycle regulation provided by PIP box-and Cul4Cdt2-mediated destruction of E2f1 during S phase. Dev Cell 2008;15:890–900. [PubMed: 19081076]

Shogren-Knaak M, Ishii H, Sun JM, Pazin MJ, Davie JR, Peterson CL. Histone H4-K16 acetylation controls chromatin structure and protein interactions. Science 2006;311:844–847. [PubMed: 16469925]

Solomon DA, Cardoso MC, Knudsen ES. Dynamic targeting of the replication machinery to sites of DNA damage. J Cell Biol 2004;166:455–463. [PubMed: 15314062]

Soria G, Gottifredi V. PCNA-coupled p21 degradation after DNA damage: The exception that confirms the rule? DNA Repair (Amst) 2010;9:358–364. [PubMed: 20060369]

Tardat M, Murr R, Herceg Z, Sardet C, Julien E. PR-Set7-dependent lysine methylation ensures genome replication and stability through S phase. J Cell Biol 2007;179:1413–1426. [PubMed: 18158331]

Vermeulen M, Mulder KW, Denissov S, Pijnappel WW, van Schaik FM, Varier RA, Baltissen MP, Stunnenberg HG, Mann M, Timmers HT. Selective anchoring of TFIID to nucleosomes by trimethylation of histone H3 lysine 4. Cell 2007;131:58–69. [PubMed: 17884155]

Warbrick E. PCNA binding through a conserved motif. Bioessays 1998;20:195–199. [PubMed: 9631646]

Yin Y, Yu VC, Zhu G, Chang DC. SET8 plays a role in controlling G1/S transition by blocking lysine acetylation in histone through binding to H4 N-terminal tail. Cell Cycle 2008;7:1423–1432. [PubMed: 18418072]

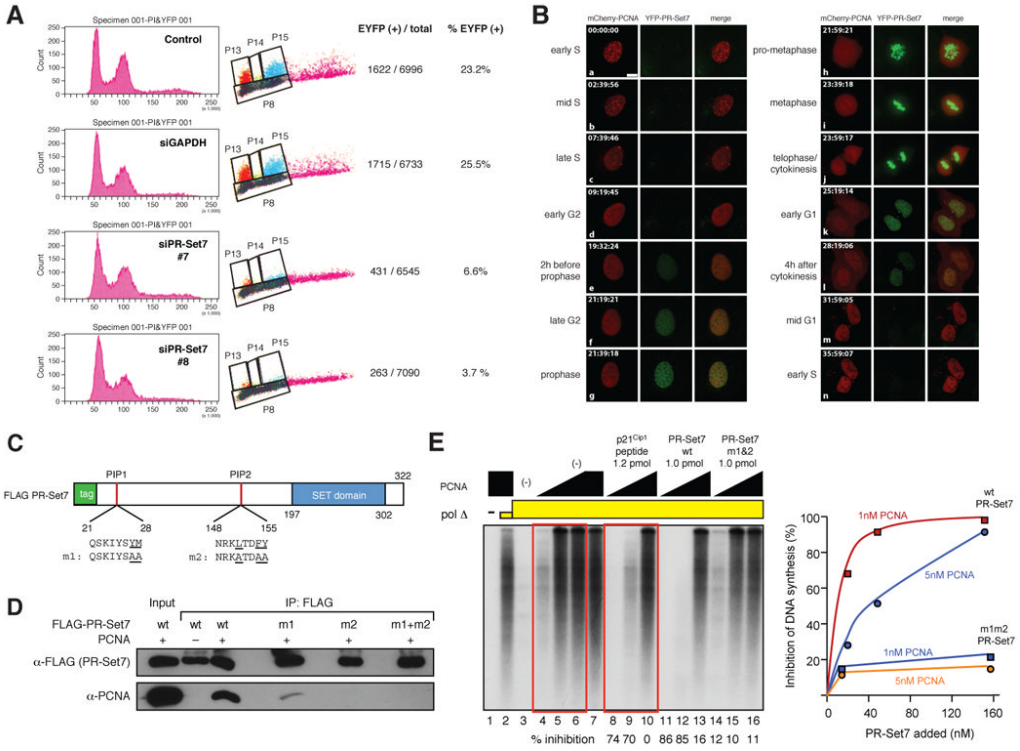

Figure 1. PR-Set7 is undetectable in S phase and interacts with PCNA *in vitro*

(A) FACS analysis of U2OS cells stably expressing EYFP-PR-Set7. The Y-axis shows cell count and fluorescence intensity of EYFP derived from EYFP-PR-Set7. The X-axis represents DNA content. The majority of positive cells were observed at G1 and G2/M, but hardly detectable during S phase. si-RNAs of PR-Set7 reduce the number of cells which have a EYFP signal (*bottom two panels*).

(B) Single cell time-lapse analysis reveals that YFP-PR-Set7 is undetectable during S phase, but detectable from late G2 through mitosis to early G1. S-phase is visualized by mCherry-PCNA labeling of replication foci. YFP-PR-Set7, green; mCherry-PCNA, red; representative data of n=35 cells is shown; scale bar, 5 μm.

(C) Schematic of recombinant human PR-Set7 protein used for protein interaction assays. Two PIP domains (PIP1 and PIP2) are depicted with their amino acid sequences shown below; amino acids changed in the PIP mutants m1 and m2 are underlined. N-terminal FLAG-tag and SET domain are shown by rectangles in green and blue, respectively.

(D) PR-Set7 interacts with PCNA in a PIP domain dependent manner. Western blot analysis using anti-FLAG immunoprecipitations performed with purified recombinant FLAG-tagged PR-Set7, either wild type or mutant in the PR-Set7 PIP domains, and purified recombinant PCNA.

(E) PR-Set7 can inhibit PCNA dependent DNA polymerization *in vitro*, in a PIP domain dependent manner. PR-Set7, as well as p21, inhibits nucleotide incorporation by DNA polymerase δ in a DNA polymerization assay performed *in vitro*. The area outlined in red rectangles shows corresponding lanes in which the same incremental amounts of PCNA were used in the assay. On the right: Graph of percentage inhibition of DNA synthesis calculated from the results shown in (E).

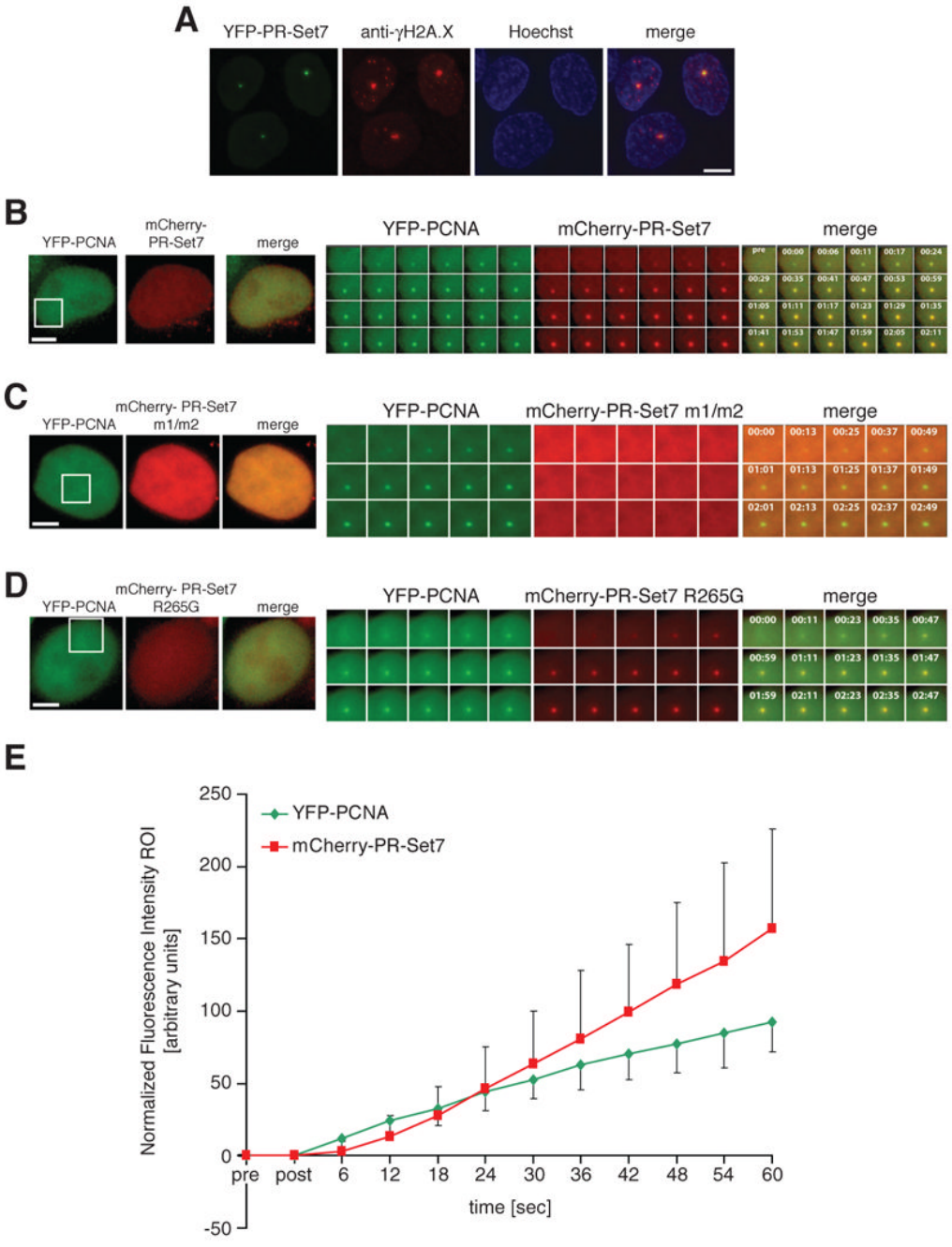

Figure 2. PR-Set7 is recruited to DNA damage sites in a PCNA dependent manner

(A) PR-Set7 co-localizes with γ-H2A.X foci at sites of laser-induced DNA damage. YFP-PR-Set7, green; anti-γ-H2A.X immunolabeling, red; Hoechst DNA labeling, blue; representative data of n=21 cells is shown; scale bar, 5 μm.

(B) PCNA and PR-Set7 are recruited to DNA damage sites. YFP-PCNA, green; mCherry-PR-Set7, red; time post irradiation in sec; representative data of n=30 cells is shown; scale bar, 5 μm; the enlarged area is indicated by a white square.

(C) PIP domains of PR-Set7 are essential for its recruitment to DNA damage sites. YFP-PCNA, green; mCherry-PR-Set7 m1/m2, red; representative data of n=8 cells is shown; scale bar, 5 μm

(D) Catalytic activity of PR-Set7 is dispensable for its recruitment to DNA damage sites. YFP-PCNA, green; mCherry-PR-Set7 R265G, red; representative data of n=8 cells is shown; scale bar, 5 μm.
(E) Quantification of mCherry-PR-Set7 and YFP-PCNA recruitment to a DNA damage site. Average fluorescence intensities of the ROI over background, arbitrary units; error bars, standard deviation (n=7).

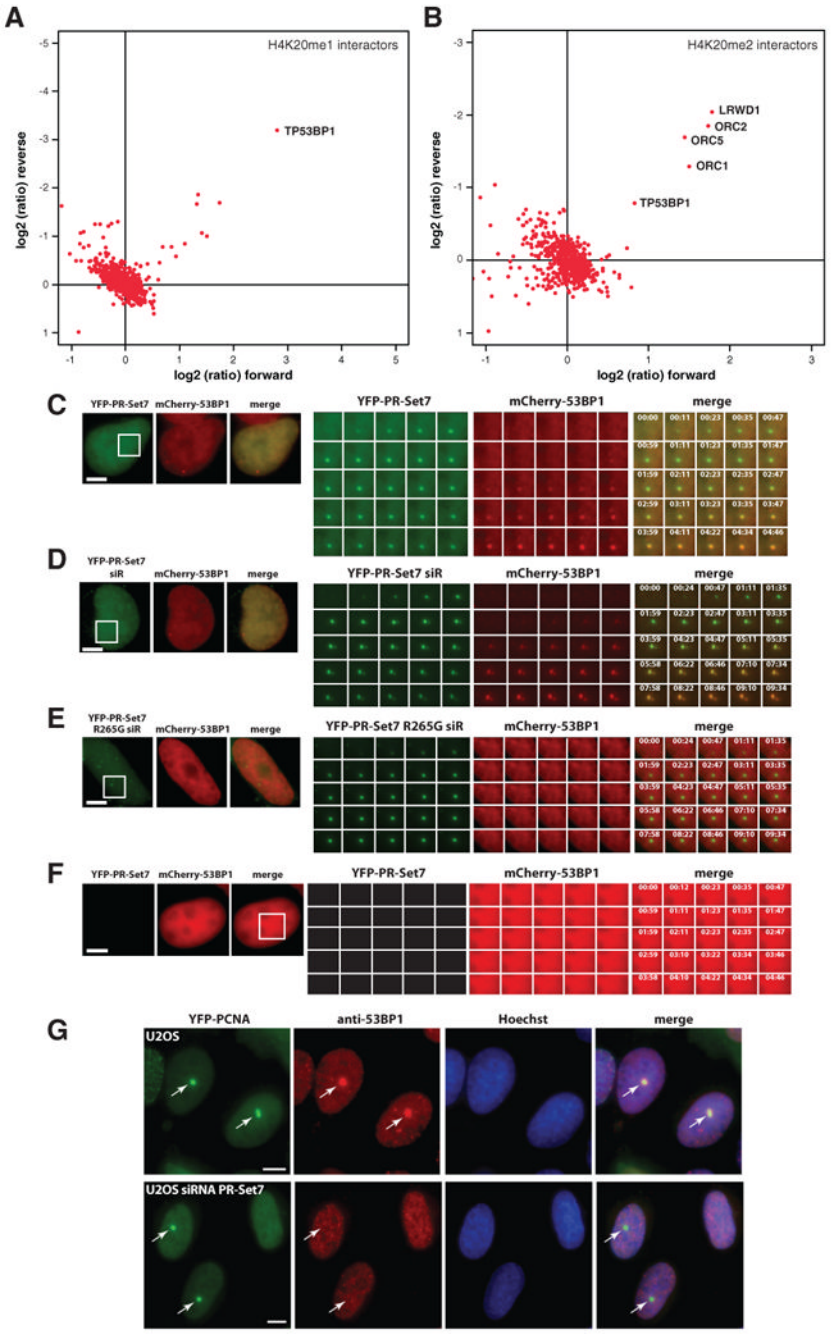

Figure 3. PR-Set7 catalytic activity is required for 53BP1 recruitment to a DNA damage site

(A) 53BP1 binds H4K20me1, as determined by a SILAC-based histone peptide pull-down approach. Proteins are plotted according to their SILAC-ratio in the "forward" (x-axis; unmodified peptide incubated with "light" extract, modified peptide incubated with "heavy" extract) and "reverse" (y-axis; unmodified peptide incubated with "heavy" extract, modified peptide incubated with "light" extract) experiment. Specific interactors should lie close to the diagonal in the upper right quadrant. Background binders cluster together in the bottom left part of the graph, showing a 1:1 ratio in both experiments.

(B) 53BP1 binds H4K20me2, as determined by a SILAC-based histone peptide pull-down approach. Plot is as described in (A).

(C) PR-Set7 recruitment to a DNA damage site precedes that of 53BP1. YFP-PR-Set7, green; mCherry-53BP1, red; representative data of n=8 cells is shown; scale bar, 5 μm.
(D) Cells treated with siRNA against PR-Set7 exhibit similar 53BP1 recruitment to a DNA damage site as in (B), upon transient expression of siRNA resistant WT PR-Set7. YFP-PR-Set7 siR, green; mCherry-53BP1, red; representative data of n=7 cells is shown; scale bar, 5 μm
(E) In contrast to (C), siRNA-PR-Set7 treated cells are devoid of detectable 53BP1 recruitment to a DNA damage site upon transient expression of the catalytically inactive PR-Set7 mutant (R265G). YFP-PR-Set7 R265G, green; mCherry-53BP1, red; representative data of n=8 cells is shown; scale bar, 5 μm.
(F) PR-Set7 is required for 53BP1 binding to the DNA damage site. Cells treated with PR-Set7 siRNA for 3 days were transfected with mCherry-53BP1. YFP-PR-Set7, green; mCherry-53BP1, red; representative data of n=10 cells is shown; scale bar, 5 μm.
(G) Recruitment of endogenous 53BP1 to a DNA damage site requires PR-Set7. U2OS cells expressing YFP-PCNA were mock treated or transfected for 3 days with siRNA against PR-Set7. Cells were fixed 6 min after the laser pulse and subjected to immunofluorescence labeling of endogenous 53BP1. YFP-PCNA, green; anti-53BP1, red; Hoechst DNA labeling, blue; arrows indicate the irradiated site; representative data of n=6 (U2OS) or n=10 (U2OS siRNA PR-Set7) cells is shown; scale bar, 5 μm.

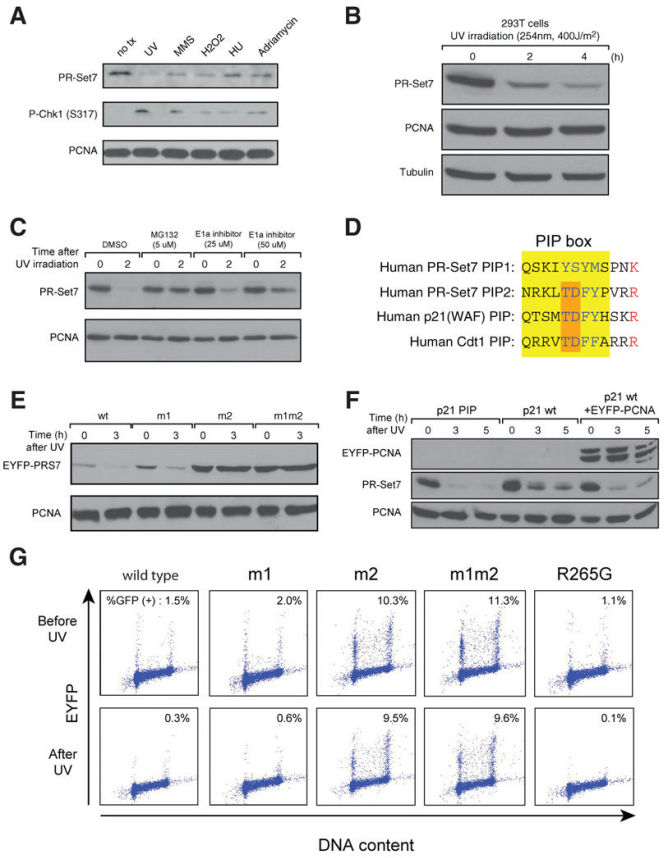

Figure 4. The PIP2 domain is required for PR-Set7 degradation during the cell cycle and after UV irradiation

(A) PR-Set7 protein levels decreased after treating U2OS cells with a panel of DNA damaging agents, as follows: UV irradiation (400 J/m^2), MMS (3mM, 1 hr), H2O2 (500uM, 30m), HU (1mM, 16 hr), and Adriamycin (1 μg/ml, 4 hr). Phospho-Chk1-serine 317 served as a marker for DNA damage, and PCNA as a loading control.

(B) The protein levels of PR-Set7 decrease after UV irradiation (400 J/m^2) in HEK293T cells as analyzed by western blotting. Both PCNA and β-tubulin serve as loading controls.

(C) UV-treated HEK293T cells exhibit increased PR-Set7 levels in the presence of proteasome inhibitor or ubiquitin activating enzyme E1 inhibitor.

(D) Comparison of PR-Set7 PIP sites with other PIP degron containing proteins. Amino acid residues of the PIP box are highlighted in yellow. The TD residues and a basic amino acid at +4 (red) in the PIP degron are conserved between the PR-Set7 PIP2 and PIP degrons of human p21 and Cdt1.

(E) PR-Set7 mutant in its PIP2 domain (m2 or m1/m2) does not exhibit degradation after UV irradiation, relative to PR-Set7 either wild type or mutant in its PIP1 domain (m1).

(F) Overexpression of wild type p21, but not its PIP mutant, attenuates PR-Set7 degradation in UV-treated HEK293T cells. PR-Set7 degradation is restored upon co-expressing EYFP-PCNA protein with wild type p21.

(G) FACS analysis of cells expressing EYFP-tagged PR-Set7, either wild type or mutant in one (m1 or m2) or both (m1/m2) PIP domains, or catalytically inactive (R265G), as a function of UV-treatment (400 J/m^2). Irrespective of UV-treatment, GFP positive cells expressing PR-Set7 mutant in PIP2 are more abundant.

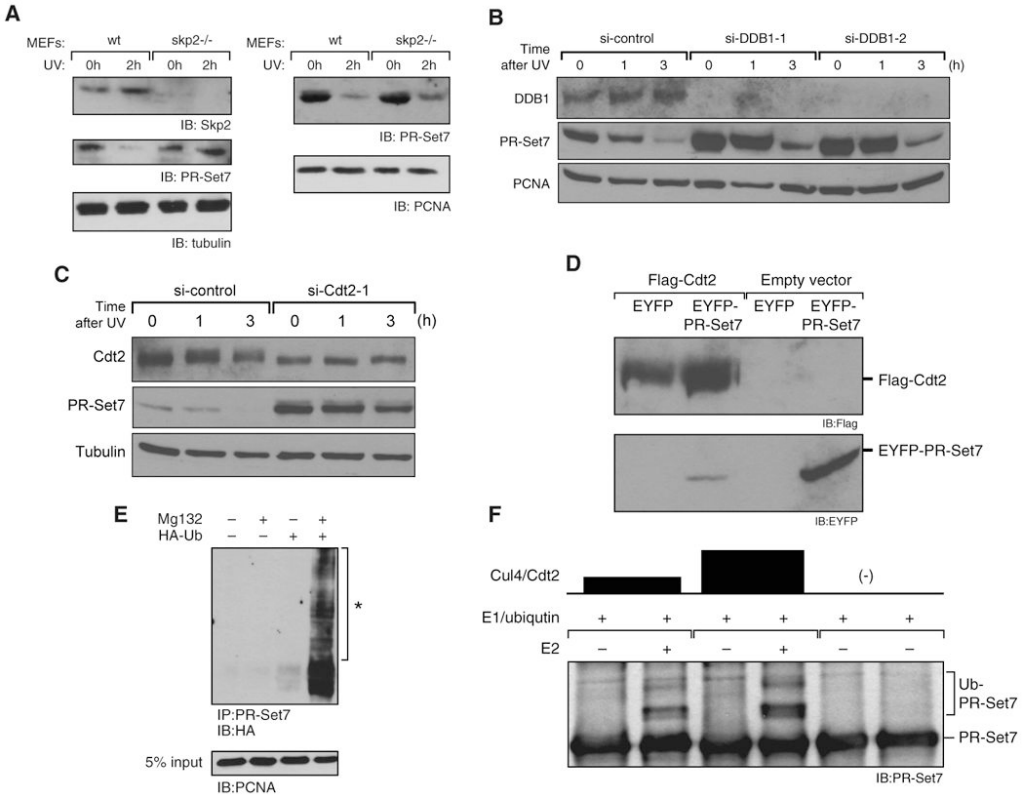

Figure 5. PR-Set7 is degraded by the CRL4^{Cdt2} ubiquitin ligase

(A) Loss of Skp2 shows partial stabilization of PR-Set7 after UV treatment. PR-Set7 protein levels were analyzed in both *Skp2*$^{-/-}$ and wild type MEFs after UV treatment. Western blot analysis of the levels of PR-Set7 in whole cell extracts (left side) and in chromatin bound proteins (right side). Tubulin and PCNA serve as loading controls, respectively.

(B) siRNA mediated knockdown of DDB1 results in PR-Set7 accumulation irrespective of UV-treatment. Western blot of chromatin fraction derived from non-irradiated or UV-irradiated (400 J/m^2) 293T cells after DDB1 knockdown. PCNA served as a loading control.

(C) siRNA mediated knockdown of Cdt2 prevents PR-Set7 degradation irrespective of UV treatment. Similar experiment as in (B), using tubulin as a loading control.

(D) Transient expression levels of EYFP-PR-Set7 are reduced upon co-transfection with FLAG-Cdt2 in 293T cells.

(E) Endogenous PR-Set7 is polyubiquitylated *in vivo* after treatment with MG132. Western blot analysis using anti-HA antibody of endogenous PR-Set7 immunoprecipitated from 293T cells after transfection with HA-Ubiquitin,. Polyubiquitylated PR-Set7 is indicated with an asterisk.

(F) CRL4^{Cdt2} E3 ligase ubiquitylates PR-Set7. Results from an ubiquitylation assay performed *in vitro* using affinity purified CRL4^{Cdt2} and recombinant PR-Set7. Ubiquitin-conjugated PR-Set7 (Ub-PR-Set7).

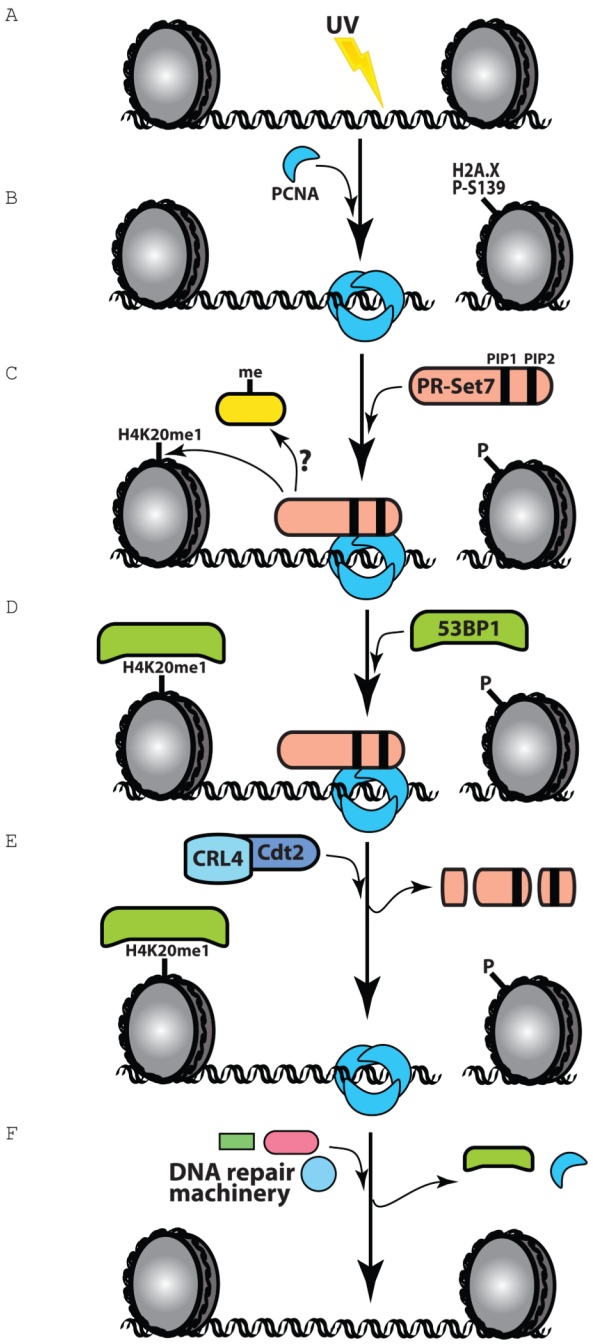

Figure 6. Model for Regulation of PR-Set7 at DNA Damage sites

(A) DNA damage induces H2A.X phosphorylation, and PCNA gets recruited to the DNA damage site

(B) PR-Set7 binds to PCNA through its PIP domains (via interaction through PIP1 and/or PIP2)

(C) PR-Set7 methylates H4K20, and possibly other non-histone proteins.

(D) 53BP1 binds to monomethylated lysine H4K20 through its double Tudor domains.

(E) $CRL4^{Cdt2}$ ubiquitylates PR-Set7 through the interaction with PIP2, followed by proteasomal degradation.

(F) PCNA remains at the DNA damage site and works as a platform to recruit other repair proteins.